NASA TECHNICAL NOTE

NASA TN D-6784



NASA TN D-6784

# EFFECTS OF ECCENTRICITIES AND LATERAL PRESSURE ON THE DESIGN OF STIFFENED COMPRESSION PANELS

*by Gary L. Giles and Melvin S. Anderson*

*Langley Research Center*
*Hampton, Va. 23365*



NATIONAL AERONAUTICS AND SPACE ADMINISTRATION • WASHINGTON, D. C. • JUNE 1972

| 1. Report No. | 2. Government Accession No. | 3. Recipient's Catalog No. |
|---|---|---|
| NASA TN D-6784 | | |

4. Title and Subtitle
EFFECTS OF ECCENTRICITIES AND LATERAL PRESSURE ON THE DESIGN OF STIFFENED COMPRESSION PANELS

5. Report Date
June 1972

6. Performing Organization Code

7. Author(s)
Gary L. Giles and Melvin S. Anderson

8. Performing Organization Report No.
L-6547

9. Performing Organization Name and Address
NASA Langley Research Center
Hampton, Va. 23365

10. Work Unit No.
134-14-05-02

11. Contract or Grant No.

12. Sponsoring Agency Name and Address
National Aeronautics and Space Administration
Washington, D.C. 20546

13. Type of Report and Period Covered
Technical Note

14. Sponsoring Agency Code

15. Supplementary Notes

16. Abstract

An analysis for determining the effects of eccentricities and lateral pressure on the design of stiffened compression panels is presented. The four types of panel stiffeners considered are integral, zee, integral zee, and integral tee. Mass-strength curves, which give the mass of the panel necessary to carry a specified load, are given along with related design equations needed to calculate the cross-sectional dimensions of the minimum-mass-stiffened panel. The results of this study indicate that the proportions of the panels are geometrically similar to the proportions of panels designed for no eccentricity or lateral pressure, but the cross-sectional dimensions are greater, resulting in significantly increased mass.

The analytical minimum-mass designs of zee-stiffened panels are compared with designs from experimentally derived charts. An assumed eccentricity of 0.001 times the length of the panel is used to correlate the analytical and experimental data. Good correlation between the experimentally derived and the analytical curves is obtained for the range of loading where material yield governs the design. At lower loads the mass given by the analytical curve using this assumed eccentricity is greater than that given by the experimental results.

| 17. Key Words (Suggested by Author(s)) | 18. Distribution Statement |
|---|---|
| Eccentrically loaded panels<br>Minimum-mass panels | Unclassified – Unlimited |

| 19. Security Classif. (of this report) | 20. Security Classif. (of this page) | 21. No. of Pages | 22. Price* |
|---|---|---|---|
| Unclassified | Unclassified | 33 | $3.00 |

*For sale by the National Technical Information Service, Springfield, Virginia 22151

# EFFECTS OF ECCENTRICITIES AND LATERAL PRESSURE ON THE DESIGN OF STIFFENED COMPRESSION PANELS

By Gary L. Giles and Melvin S. Anderson
Langley Research Center

## SUMMARY

An analysis for determining the effects of eccentricities and lateral pressure on the design of stiffened compression panels is presented. The four types of panel stiffeners considered are integral, zee, integral zee, and integral tee. Mass-strength curves, which give the mass of the panel necessary to carry a specified load, are given along with related design equations needed to calculate the cross-sectional dimensions of the minimum-mass-stiffened panel. The results of this study indicate that the proportions of the panels are geometrically similar to the proportions of panels designed for no eccentricity or lateral pressure, but the cross-sectional dimensions are greater, resulting in significantly increased mass.

The analytical minimum-mass designs of zee-stiffened panels are compared with designs from experimentally derived charts. An assumed eccentricity of 0.001 times the length of the panel is used to correlate the analytical and experimental data. Good correlation between the experimentally derived and the analytical curves is obtained for the range of loading where material yield governs the design. At lower loads the mass given by the analytical curve using this assumed eccentricity is greater than that given by the experimental results.

## INTRODUCTION

The design of efficient aerospace structures requires the sizing of individual structural components to have low mass with maximum strength. Stiffened panels which are used on the upper surface of airplane wings or in the interstage and intertank structures of launch vehicles, where the primary loading is uniaxial compression, are an important class of components which have been studied extensively. Mass-strength curves which give the mass of the stiffened panel required to carry a given applied load have been obtained previously by assuming that the compressive load is applied through the neutral surface of the panel. (See ref. 1.) In most practical designs, it is nearly impossible to achieve a panel loading that is not eccentric because of imperfections in the panel, and in some designs other considerations necessitate the intentional application of panel end loads which are eccentric to the neutral surface. In many designs compression panels are also acted on by lateral pressure. Design procedures for stiffened panels often

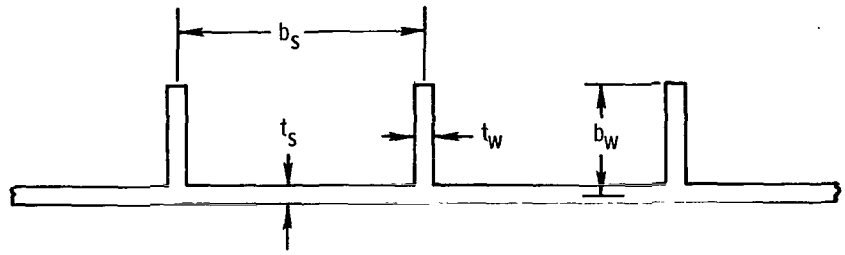


Integral stiffened

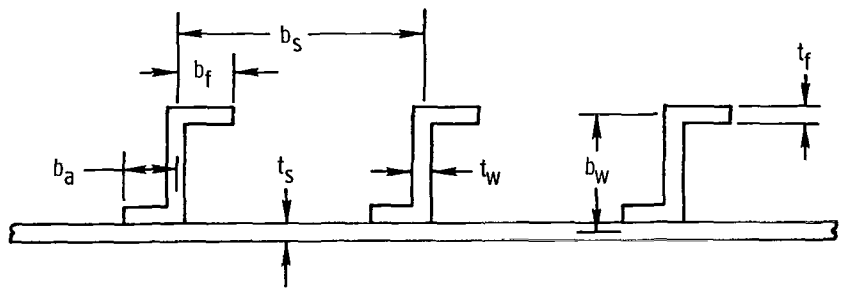


Zee stiffened

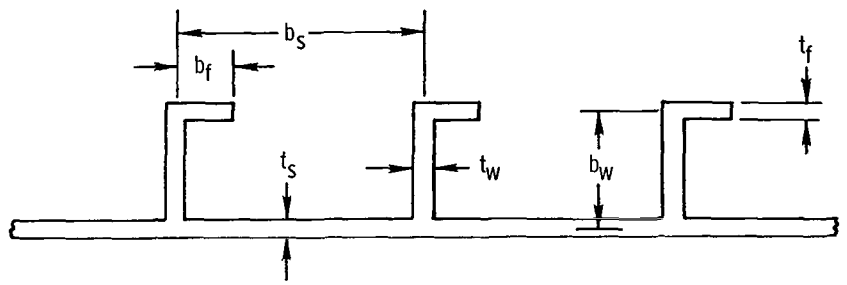


Integral - zee stiffened

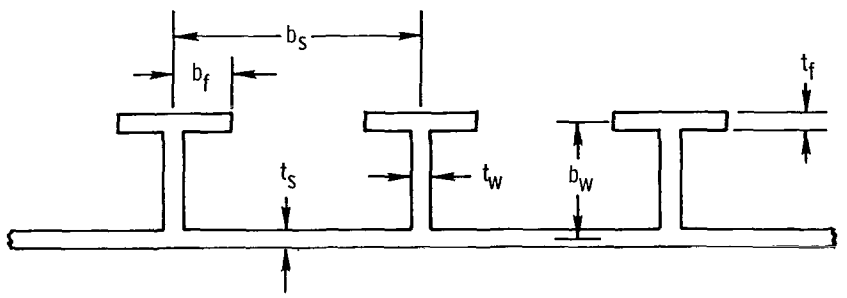


Integral - tee stiffened

Figure 1.- Cross section of stiffened compression panels.

account for eccentricities and lateral pressure only through the use of experience factors. However, a method for designing eccentrically loaded thin-walled round columns has been developed in reference 2, and a similar rational approach to the design of stiffened compression panels which includes the effects of eccentricities and lateral pressure is needed.

An analysis is presented for determining minimum-mass proportions of four types of stiffened panels for a range of eccentrically applied uniaxial compressive end loads. Equivalence relationships are established which relate the design parameters for panels with initial imperfections and lateral pressure to the design parameter for panels under eccentric end loading. Thus the data presented in this report can be used to account for all three of these effects during the design of stiffened panels. The four types of panel stiffeners (fig. 1) considered are integral, zee, integral zee, and integral tee. Mass-strength curves along with related design equations needed to calculate the cross-sectional dimensions of these stiffened panels are presented. For the zee-stiffened panels, the analytical minimum-mass designs are compared with designs from experimentally derived charts.

## SYMBOLS

| | |
|---|---|
| $A$ | cross-sectional area per unit width of panel |
| $a$ | maximum amplitude of initial imperfection of sinusoidal shape denoted by $a \sin \frac{\pi x}{l}$ |
| $B, B_1$ | dimensionless parameters defined by equations (A23) and (A24), respectively |
| $b_a, b_f, b_s, b_w$ | width of attachment, flange, and skin segments and depth of web segment of panel cross section, respectively (see fig. 1) |
| $c$ | distance from neutral surface to location where stress is to be calculated (see eq. (1)) |
| $E$ | Young's modulus for material |
| $E_S$ | secant modulus for material at given stress |
| $E_T$ | tangent modulus for material at given stress |
| $e$ | load eccentricity measured from neutral surface of stiffened panel (positive toward skin) |

| | |
|---|---|
| H | constant (see eq. (A14)) |
| I | area moment of inertia |
| k | local buckling coefficient |
| $l$ | panel length |
| M | bending moment |
| $N_x$ | axial compressive load per unit width of panel |
| n | constant (equals 0, 1, or 2 for integral-stiffened, zee- and integral-zee-stiffened, and integral-tee-stiffened panels, respectively) |
| P | axial compressive load |
| q | lateral pressure load |
| R | geometric ratio, $\frac{b_f}{b_w}\frac{t_f}{t_w}$ |
| $r_b$ | ratio of depth of web to width of skin, $b_w/b_s$ |
| $r_t$ | ratio of thicknesses, $t_w/t_s$ |
| $\bar{t}$ | mass-equivalent flat-plate thickness of a stiffened panel |
| $t_f, t_s, t_w$ | thickness of flange, skin, and web segments of cross section, respectively (fig. 1) |
| x | distance along length of panel |
| y | distance normal to panel |
| $y_o$ | distance from neutral surface of plate-stiffener combination to middle surface of skin |
| $\alpha$ | dimensionless parameter defined by equation (A12) |

$\beta$ dimensionless parameter defined by equation (A13)

$\gamma$ constant selected to establish equivalence between panel with initial imperfection and panels with eccentric end load or lateral pressure

$\epsilon$ structural efficiency factor

$\eta_g$ plasticity reduction factor for general buckling defined by equation (A8)

$\eta_l$ plasticity reduction factor for local buckling defined by equation (A10)

$\theta$ dimensionless parameter, $\beta \frac{l}{b_w}$

$\mu$ Poisson's ratio

$\xi_1, \xi_2, \xi_3$ geometric parameters defined by equations (A2), (A4), and (A6), respectively

$\rho$ radius of gyration of panel cross section

$\sigma$ stress

$\sigma_{av}$ average applied compressive stress, $N_x/\bar{t}$

$\sigma_{cy}$ material compressive-yield stress

$\sigma_E$ Euler column-buckling stress, $\pi^2 E\left(\frac{\rho}{l}\right)^2$

$\sigma_l$ local buckling stress

$\sigma_{max}$ maximum compressive stress in panel cross section

$\phi$ equivalent-eccentricity parameter defined by equation (5)

## BEAM-COLUMN BEHAVIOR OF COMPRESSION PANELS

In this report the compression panels are analyzed as wide columns by assuming that the panels are of sufficiently small curvature and of sufficient width to render the buckling load independent of curvature and boundary conditions along the unloaded edges. The three loading conditions of eccentrically applied end load, initial imperfection, and

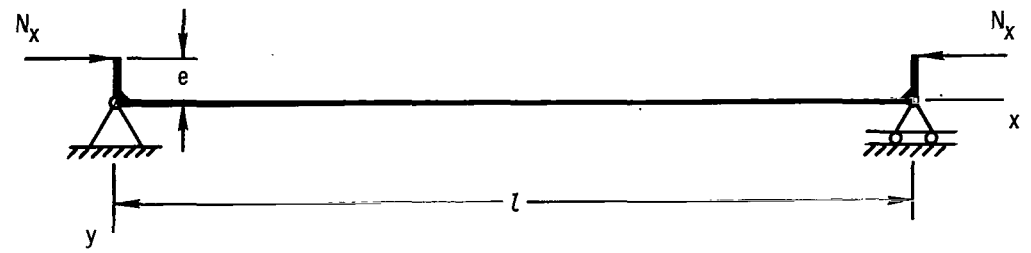


Eccentric end load

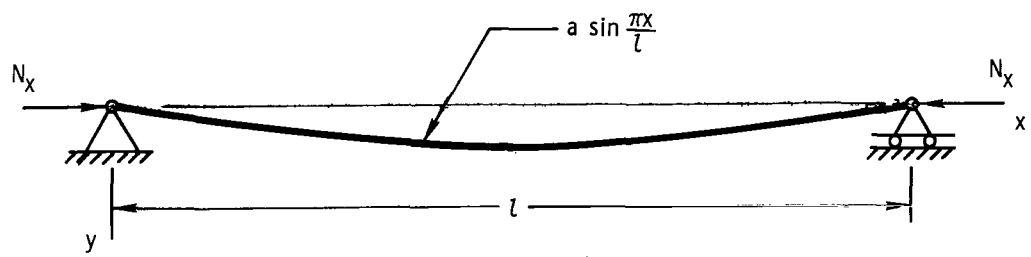


Initial imperfection

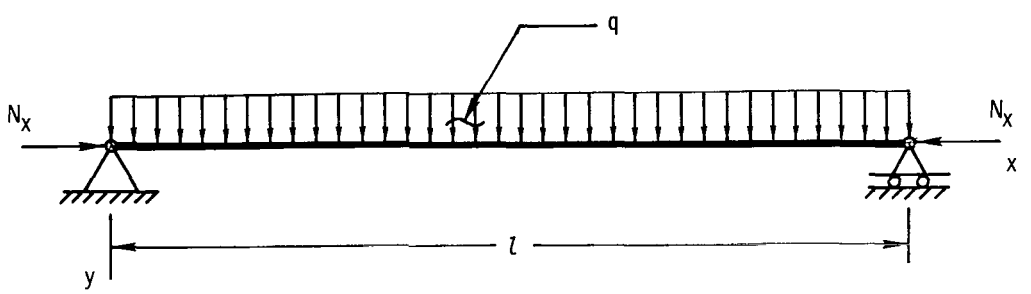


Lateral pressure

Figure 2.- Schematic of loading conditions.

lateral pressure, shown in figure 2, are considered. As indicated, a sine wave was selected as the shape of the initial imperfection, and the pressure loading is constant over a panel. Stresses acting on a panel cross section are the superposition of the direct stress from the applied load and the stress resulting from the moment which is produced by the eccentric application of the load or the lateral pressure. The magnitude of the stress is given by

$$\sigma = \frac{P}{A} + \frac{Mc}{I} \tag{1}$$

The maximum value of stress $\sigma$ occurs at the midlength of the panel $\left(x = \frac{l}{2}\right)$ and differs for each of the three loading conditions only by the difference in expressions for the bending moment M. Expressions for the maximum bending moment corresponding to each of the conditions are derived in reference 3. The expressions in nondimensionalized form are

For eccentric end load

$$\frac{M}{N_x l\left(\frac{e}{l}\right)} = \sec\left(\frac{\pi}{2}\sqrt{\frac{\sigma_{av}}{\sigma_E}}\right) \tag{2}$$

For initial imperfection

$$\frac{M}{N_x l\left(\frac{1}{\gamma}\frac{a}{l}\right)} = \frac{\gamma}{1 - \frac{\sigma_{av}}{\sigma_E}} \tag{3}$$

For lateral pressure

$$\frac{M}{N_x l\left(\frac{ql}{N_x}\right)} = \frac{\sec\left(\frac{\pi}{2}\sqrt{\frac{\sigma_{av}}{\sigma_E}}\right) - 1}{\sigma_{av}/\sigma_E} \tag{4}$$

The equations were written in the nondimensionalized form shown to establish equivalence relationships between the design parameters of $e/l$ for the eccentrically end-loaded panels, $\frac{1}{\gamma}\frac{a}{l}$ for panels with initial imperfections, and $ql/N_x$ for panels under lateral pressure. The nondimensional moments are related to the ratio of the average stress to the Euler buckling stress of the panel $\sigma_{av}/\sigma_E$, and these relationships are compared graphically in figure 3. The curves exhibit a similar trend for the entire range of loading $\sigma_{av}/\sigma_E$. For practical values of eccentricity or lateral pressure, efficient panel design is obtained for $\frac{\sigma_{av}}{\sigma_E} > 0.5$. In this range the moment curves for panels with eccentric end loads and lateral pressure are in very good agreement. The constant multiplier $\gamma$ is introduced to provide correlation between the curve for panels with an initial imperfection and the other two curves. The curve for $\gamma = 1.0$ is shown in figure 3. When $\gamma = 1.25$ is used, the curve for initial imperfection cannot be distinguished from the curve for lateral pressure. Since these moment curves are in such good agreement, an equivalent-eccentricity parameter can be used to correlate the effects of all three conditions. This

equivalent-eccentricity parameter, which can be used for the design of panels with a combination of eccentricities and lateral pressure, is expressed as

$$\phi = \frac{e}{l} + \frac{1}{\gamma}\frac{a}{l} + \frac{ql}{\pi^2 N_x} \tag{5}$$

where $\gamma = 1.25$ is recommended for the initial-imperfection term.

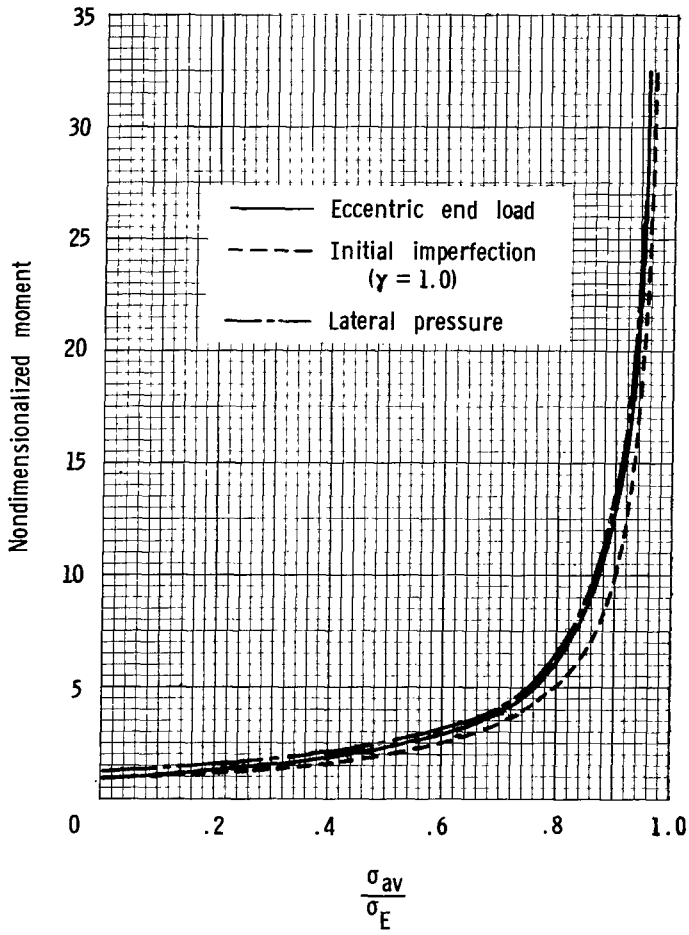


Figure 3.- Comparison of nondimensionalized moments over the range of applied stress for the loading conditions shown in figure 2.

The results derived in the appendix are for the condition of eccentric end loading where $\phi = \frac{e}{l}$. The corresponding design curves are presented in terms of the equivalent-eccentricity parameter $\phi$. (See eq. (5).) Hence, the design curves in this report are correct for the condition of eccentric end loading, but a few check cases confirm that these curves can also be used with very good approximation in the design of compression panels with initial imperfections and under lateral pressure. In the remainder of this

report, an "eccentrically loaded panel" will refer to a panel which has an eccentric end load, initial imperfection, lateral pressure, or some combination of these conditions.

## METHOD OF DESIGN

In this section the method used to include the effect of eccentricities and lateral pressures on the design of stiffened panels is established; details of the design procedure are described in the appendix. The conventional procedure used to obtain mass-strength curves for these stiffened panels loaded through their neutral surfaces (no eccentricity or lateral pressure) is based on the assumption that the minimum-mass panel is obtained when the various types of buckling occur simultaneously under the applied loading. This principle can be expressed as

$$\sigma_{av} = \sigma_E = \sigma_l \tag{6}$$

where $\sigma_{av}$ is the average applied compressive stress given by $N_x/\bar{t}$, $\sigma_E$ is the Euler column-buckling stress of the panel, and $\sigma_l$ is the local-buckling stress of the panel. In this report local buckling refers to buckling of the cross section of the panel and is determined using the principle of moment distribution between the elements of the cross section.

The principle given in equation (6) is not applicable to the present investigation since eccentrically loaded panels do not exhibit bifurcation (Euler) buckling. For the eccentrically loaded panel, the counterpart of the Euler buckling load can be obtained by studying the large deflection behavior of the panel. The eccentrically loaded panel exhibits a "top-of-the-knee" behavior which has been predicted theoretically by various methods summarized in reference 4. Such studies usually involve detailed knowledge of the postyielding behavior of plastically stressed columns.

For the present study an approximate method is used to avoid the complexities of such postyielding behavior. Herein the assumption is made that when the maximum stress $\sigma_{max}$ in the eccentrically loaded panel reaches a critical value, the panel has no additional load-carrying ability. The critical value is assumed to be either the compressive-yield strength of the panel material $\sigma_{cy}$ or the local-buckling strength $\sigma_l$. Thus

$$\sigma_{max} = \sigma_l \quad \text{or} \quad \sigma_{cy} \tag{7}$$

is used as the criterion for the failure of eccentrically loaded columns. While this assumption has been shown to be unduly conservative for postyielding of certain panels (ref. 4), it is likely to be a better assumption for a well-proportioned stiffened panel where significant postyielding or postbuckling strengths are unlikely.

The maximum stress is a function of the cross-section properties $\bar{t}$, $y_o$, and $\rho$, equivalent-eccentricity parameter $\phi$, panel length $l$, and the intensity of loading as expressed by the ratio of average applied stress to the Euler column-buckling stress $\sigma_{av}/\sigma_E$. In this report the moment given for the condition of the eccentric end load will be used in the equation for the maximum stress. The maximum stress can then be obtained from equations (1) and (2) as

$$\sigma_{max} = \frac{N_x}{\bar{t}}\left[1 + \frac{e}{l}\frac{y_o l}{\rho^2}\sec\left(\frac{\pi}{2}\sqrt{\frac{\sigma_{av}}{\sigma_E}}\right)\right] \tag{8}$$

which is a form of the so-called secant formula. A normalized graph of this formula is shown in figure 4, where $\sigma_{av} = \frac{N_x}{\bar{t}}$. The ordinate of the figure shows the magnification of stress produced by the equivalent-load eccentricity as a function of the ratio of average stress to Euler buckling stress $\sigma_{av}/\sigma_E$. Similar trends could be plotted for the effects of initial imperfection or lateral pressure by replacing the eccentricity parameter $e/l$ with the initial-imperfection parameter $\frac{1}{\gamma}\frac{a}{l}$ or the pressure parameter $ql/\pi^2 N_x$. For minimum-mass design, the cross section of the panel should be proportioned to make $\sigma_{av}/\sigma_E$ as large as possible. However, with eccentric loading an increase in the stress ratio $\sigma_{av}/\sigma_E$ results in a significant increase in magnification of maximum stress $\sigma_{max}/\sigma_{av}$. When the magnification of stress is large enough to produce either material yielding or to exceed the buckling stress of the panel cross section, then the panel is assumed to fail.

The criterion established for designing the panels is that local buckling or material yield and consequent failure of the panel occur simultaneously for given values of loading parameter $N_x/El$ and eccentricity parameter $\phi$. The geometric ratios of the panel cross section which provide the minimum-mass panel (minimum $\bar{t}/l$) and satisfy this design criterion are then determined. Details of the procedure are given in the appendix.

Local-buckling equations have been developed (see ref. 5, for example) for various cross sections with wide ranges of proportions. These equations were derived for a uniform stress over the cross section. Local-buckling equations are not available for cross sections under a combined compressive load and moment which results from eccentric loading. For the results presented in this report, the moment resulting from the eccentricities or lateral pressure is assumed to produce compression in the skin of the panel. The maximum stress which then occurs in the skin is the sum of the compressive stress produced by the moment and the direct compressive stress. The local-buckling behavior is then based on the conservative assumption of this maximum stress applied uniformly to the panel cross section. If local-buckling equations which account for the effects of an applied moment were developed, they could be incorporated into the present analysis.

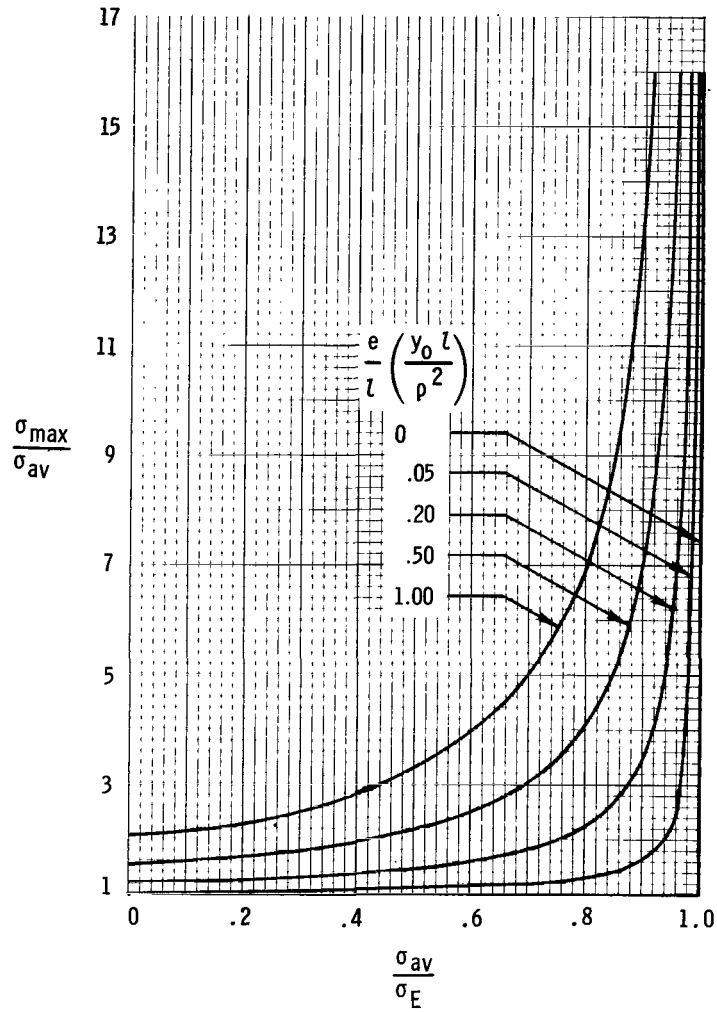


Figure 4.- Stress magnification for eccentrically loaded panels determined from $\frac{\sigma_{max}}{\sigma_{av}} = 1 + \frac{e}{l}\left(\frac{y_o l}{\rho^2}\right)\sec\frac{\pi}{2}\sqrt{\frac{\sigma_{av}}{\sigma_E}}$.

The analytical procedures discussed in this section were used to calculate design data for the integral-stiffened, integral-zee-stiffened, and integral-tee-stiffened panels for a range of loading parameters $N_x/El$ and several values of eccentricity parameter $\phi$. The analytical minimum-mass designs of zee-stiffened panels are compared with designs from experimentally derived charts. The present design data which can be used to determine both the effects of eccentricities and lateral pressure on the design of these compression panels are discussed in the following section.

## RESULTS AND DISCUSSION

Mass-strength curves for integral-stiffened, integral-zee-stiffened, and integral-tee-stiffened panels subjected to uniaxial eccentric loading are shown in figures 5 to 7,

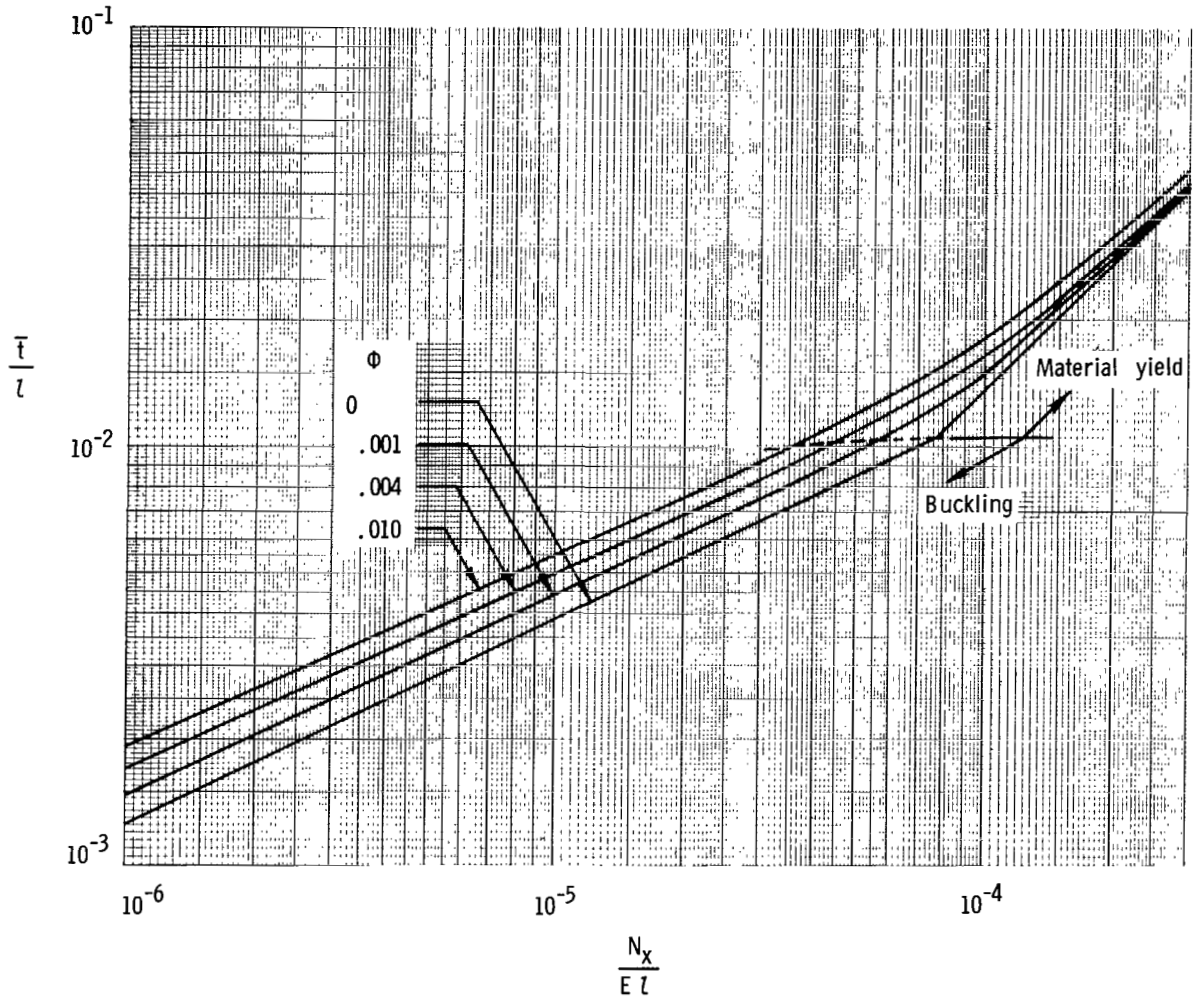


Figure 5.- Mass-strength curves for eccentrically loaded integral-stiffened panels. $\frac{\sigma_{cy}}{E} = 0.0069$.

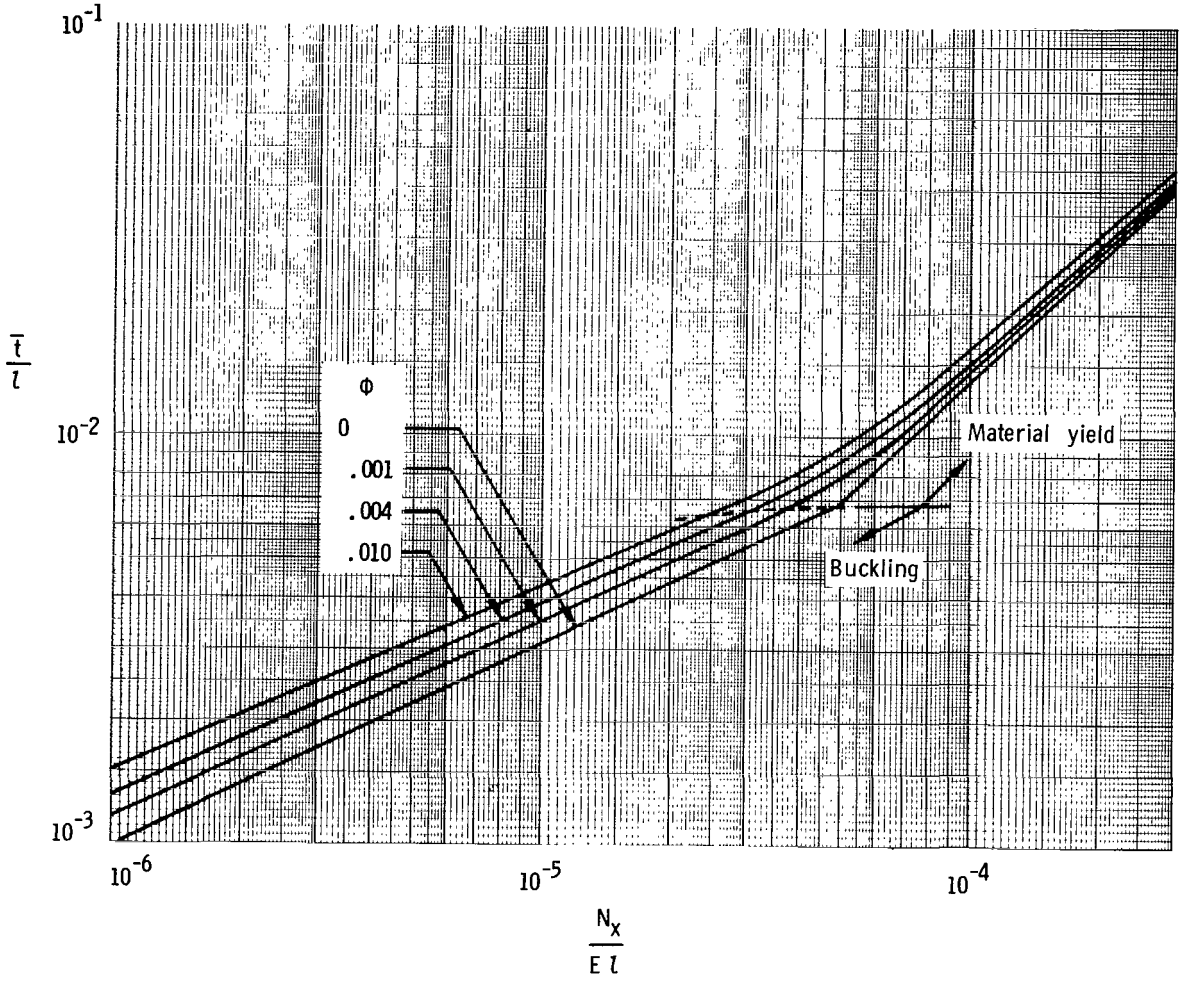


Figure 6.- Mass-strength curves for eccentrically loaded integral-zee-stiffened panels. $\frac{b_f}{b_w} = 0.3$; $\frac{t_f}{t_w} = 1.0$; $\frac{\sigma_{cy}}{E} = 0.0069$.

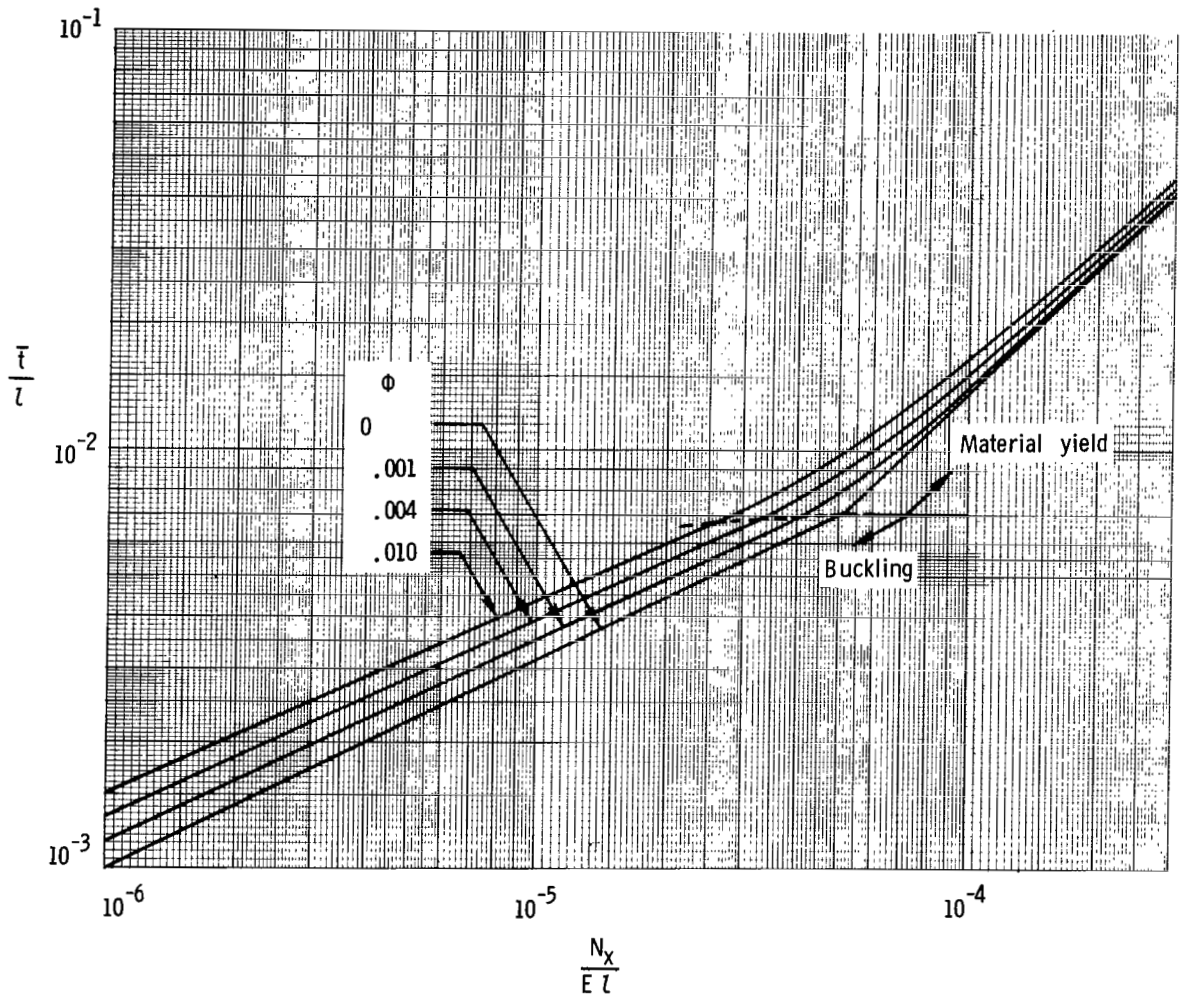


Figure 7.- Mass-strength curves for eccentrically loaded integral-tee-stiffened panels. $\frac{b_f}{b_w} = 0.3$; $\frac{t_f}{t_w} = 1.0$; $\frac{\sigma_{cy}}{E} = 0.0069$.

respectively. Results are given for only one set of commonly used flange proportions, $\frac{b_f}{b_w} = 0.3$ and $\frac{t_f}{t_w} = 1.0$. These curves give the variation of the mass-equivalent flat-plate thickness nondimensionalized by the panel length $\bar{t}/l$ with the loading parameter $N_x/El$ for several values of eccentricity parameter $\phi$. The material yield for the curves is $\frac{\sigma_{cy}}{E} = 0.0069$; this value corresponds to the material properties of 7075-T6 aluminum alloy. A dashed line separates the part of the curves which are based on buckling from the part based on material yield.

The results obtained for no eccentricity ($\phi = 0$) are shown in the appendix to agree with those obtained in reference 1. The effect of the equivalent-eccentricity parameter $\phi$ on the design of the stiffened panels at a selected load index is shown in figure 8.

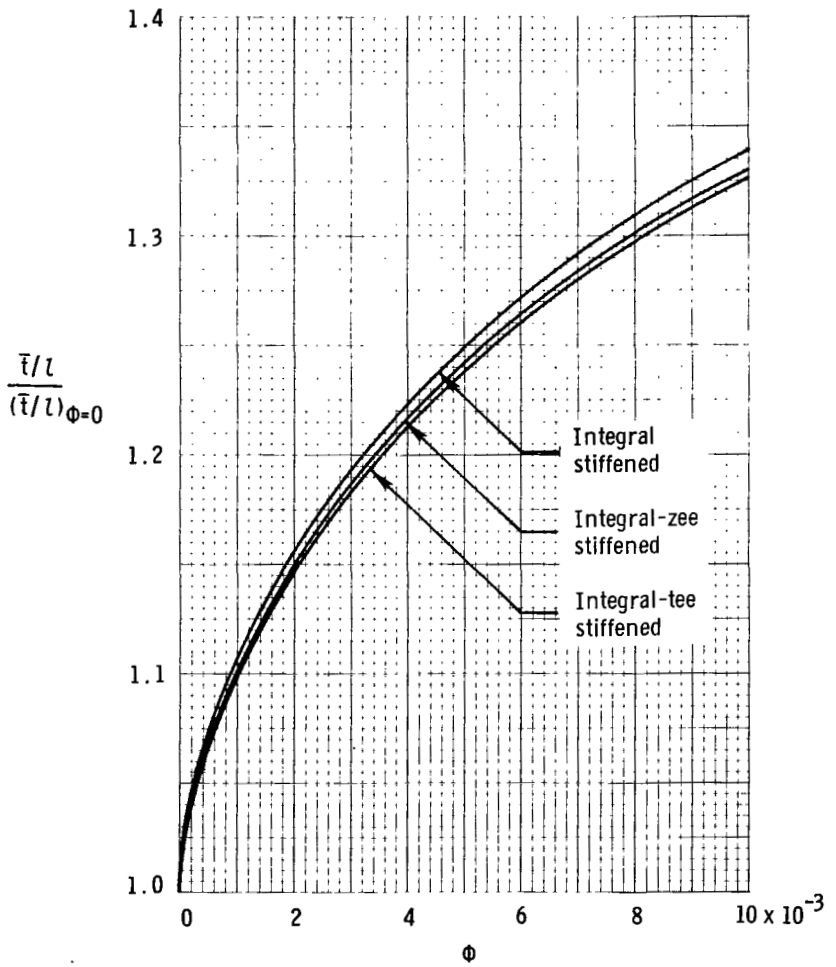


Figure 8.- Ratio of the mass parameter of eccentrically loaded panels to the mass parameter of panels under noneccentric loads for a range of the eccentricity parameter $\phi$. $\frac{N_x}{El} = 2.0 \times 10^{-5}$.

The ratio of the mass parameter for eccentrically loaded panels to the mass parameter of panels with no eccentricity is given for a range of the eccentricity parameter. In practical design, it is nearly impossible to achieve a panel loading without eccentricity effects. A significant increase in panel mass is shown to be required for even small eccentricities. Eccentricity is shown to have approximately the same effect on each of the types of stiffened panels considered. The integral-stiffened panel requires the greatest increase in mass, and the integral-tee-stiffened panel requires the least mass increase for a given value of the eccentricity parameter.

Geometric proportions of the panel cross sections corresponding to the mass-strength curves of figures 5 to 7 are given in figures 9 and 10. The optimum sets of proportions at a selected value of loading $\frac{N_x}{E\ell} = 2.0 \times 10^{-5}$ are shown for a range of eccentricity parameter $\phi$. For a given eccentricity, the variation in optimum panel proportions throughout the loading range was found to be small. Moreover, the difference in mass between panels with proportions given in figures 9 and 10 and panels with optimum proportions for other values of loading throughout the entire load range is insignificant. Therefore, these proportions shown are applicable for all loads. The optimum geometric proportions do change with eccentricity parameter $\phi$, but the changes are slight. Hence, the proportions of the panels are geometrically similar to the proportions

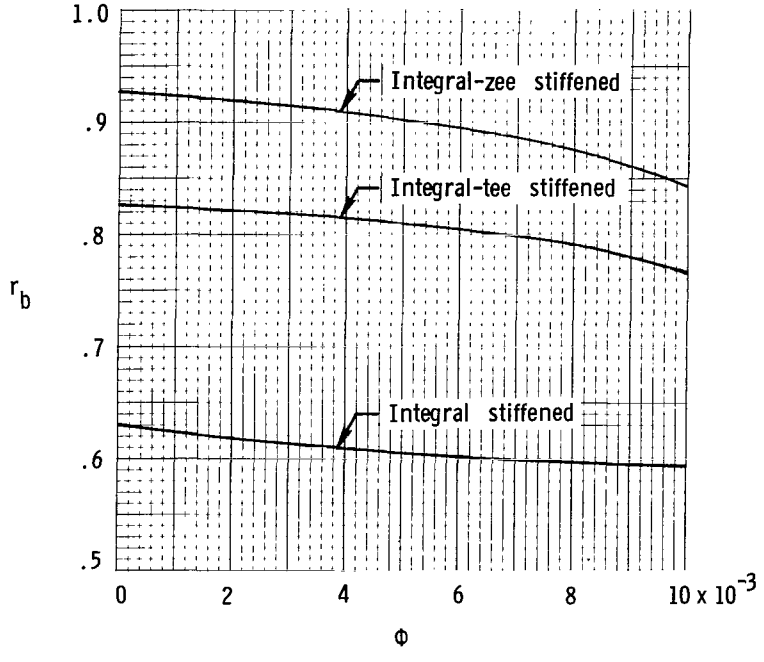


Figure 9.- Optimum ratio of depth of stiffeners to distance between stiffeners $\left(r_b = \frac{b_w}{b_s}\right)$ for eccentrically loaded panels. $\frac{N_x}{E\ell} = 2.0 \times 10^{-5}$.

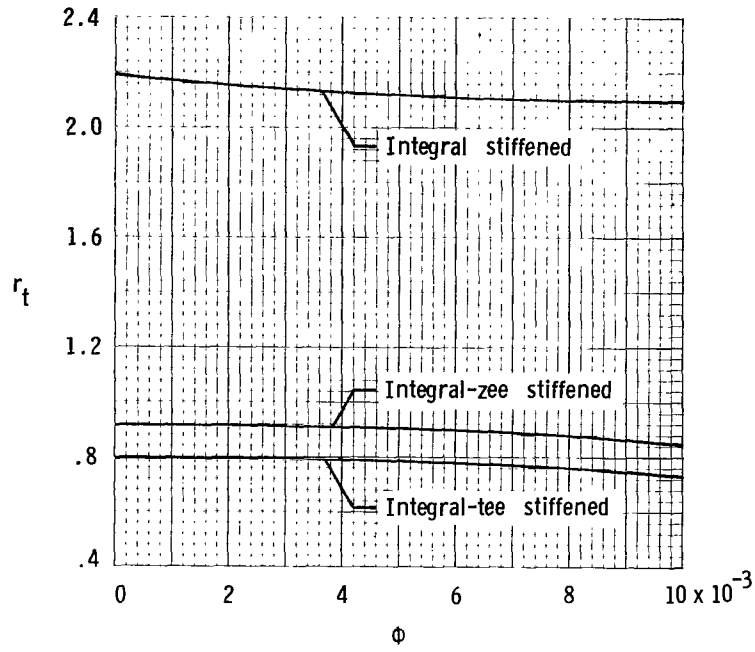


Figure 10.- Optimum ratio of stiffener thickness to skin thickness $\left(r_t = \frac{t_w}{t_s}\right)$ for eccentrically loaded panels. $\frac{N_x}{El} = 2.0 \times 10^{-5}$.

of panels designed for no eccentricities or lateral pressure, but the cross-sectional dimensions increase with increasing eccentricity parameter, resulting in an increased mass. Equations for determining the dimensions of the panel cross section at a given loading are presented in the appendix.

A mass-strength curve obtained from the experimentally derived design charts of reference 6 for a zee-stiffened panel is compared with analytical results in figure 11. The design charts are based on tests in which the intent was to load initially flat panels through their neutral surface (i.e., no eccentricities). However, the experimental results indicate that the mass of the panels required to carry a given test load is greater than that given by the analytical curve for no eccentricity of loading $\frac{e}{l} = 0$. An assumed eccentric end load of $\frac{e}{l} = 0.001$ for ideal panels is suggested in reference 3 to relate theoretical and experimental panel buckling results. An analytical mass-strength curve using this assumed value of eccentricity is also shown in figure 11. At the loading where material-yield strength governs the design, the analytical curve for $\frac{e}{l} = 0.001$ branches. One part of this curve neglects any plasticity reduction by assuming a linear stress-strain relationship up to material yield, whereas the other part uses a first-order approximation for a plasticity reduction. The first-order plasticity reduction uses the tangent modulus in the secant formula for maximum stress and uses a plasticity reduction factor from reference 7 for local buckling behavior. The nonlinear material behavior used to calcu-

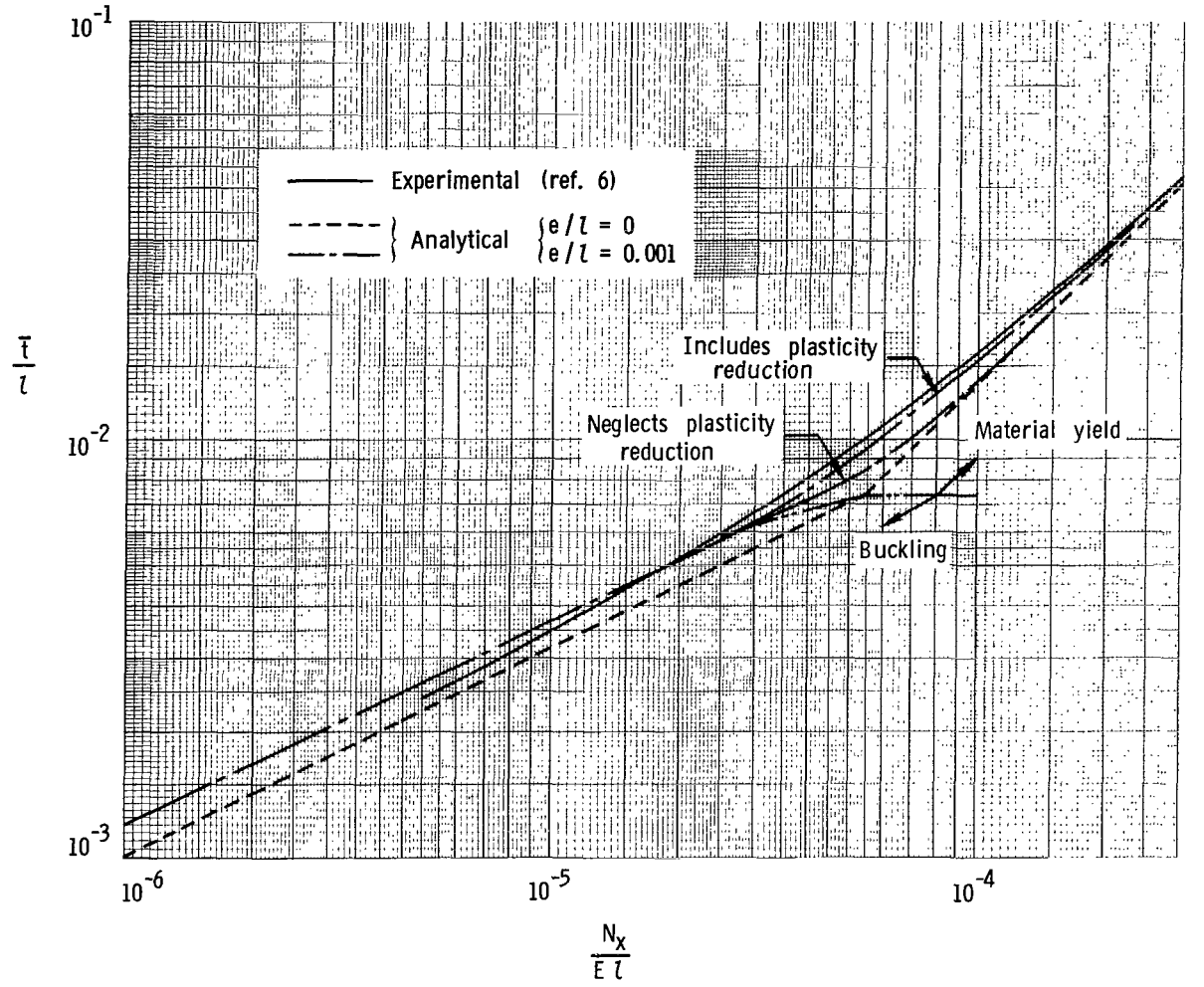


Figure 11.- Comparison of experimentally derived and analytical mass-strength curves for zee-stiffened panels. $\frac{b_f}{b_w} = 0.4$; $\frac{t_f}{t_w} = 1.0$; $\frac{b_a}{b_w} = 0.3$.

late the plasticity reduction factors were obtained from the stress-strain diagram for 7075-T6 aluminum that is presented in reference 8.

Good correlation between the experimentally derived curve and the analytical curves is obtained for the range of loading where material yield governs the design. At lower loads the analytical curve is conservative since it indicates that a greater mass than that given by the experimental curve is required to carry a given load. This conservative correlation is in part a consequence of the conservative assumptions made in the analysis. The cross-sectional proportions of specific designs based on the present analysis were compared with corresponding proportions obtained from the experimentally derived design charts of reference 6. Good correlation of the proportions was found in the high-stress range with a greater difference occurring at low values of stress. Subsequently, proportions based on the present study were used with the design charts of reference 6 to con-

struct a mass-strength curve; differences between that curve and the experimental curve shown in figure 11 were negligible.

## CONCLUDING REMARKS

An analysis for determining the effects of eccentricities and lateral pressure on the design of stiffened compression panels is presented. The four types of panel stiffeners considered are integral, zee, integral zee, and integral tee. Results are presented in terms of a single equivalent-eccentricity parameter which can be used to account for a combination of eccentric end load, initial imperfection, and lateral pressure. Mass-strength curves, which give the mass of the panel for a specified load and eccentricity parameter, are given along with related design equations needed to calculate the cross-sectional dimensions of the minimum-mass-stiffened panel. The results of this study indicate that the proportions of the panels are geometrically similar to the proportions of panels designed for no eccentricities or lateral pressure, but the cross-sectional dimensions are greater, resulting in significantly increased mass.

The analytical minimum-mass designs of zee-stiffened panels are compared with designs from experimentally derived charts. An assumed eccentricity of 0.001 times the length of the panel is used to correlate the analytical and experimental data. Good correlation between the experimentally derived and the analytical curves is obtained for the range of loading where material yield governs the design. At lower loads the mass given by the analytical curve using this assumed eccentricity is greater than that given by the experimental results.

Langley Research Center,
National Aeronautics and Space Administration,
Hampton, Va., May 3, 1972.

## APPENDIX

## MASS-STRENGTH ANALYSIS

In this appendix the mass-strength analysis of four types of stiffened panels (fig. 1) under eccentric compressive end loading is presented. The maximum compressive stress is a function of loading $N_x$, panel length $l$, eccentricity e, and the geometric proportions of the cross section.

The assumption is made that the reduction of bending stiffness of the panel when either local buckling or material yielding in the panel cross section occurs will produce failure of the panel. The criterion established for designing the panels is that local buckling or material yield and consequent failure of the panel occur simultaneously for given values of the loading parameter $N_x/El$ and the eccentricity parameter $\phi = \frac{e}{l}$. The geometric proportions of the panel cross section which provide the highest structural efficiency (lowest $\bar{t}/l$) and satisfy this design criterion are then determined.

### Geometric Properties

The mass-equivalent flat-plate thickness $\bar{t}$ nondimensionalized by the panel length $l$ is given by

$$\frac{\bar{t}}{l} = \xi_1 \frac{t_s}{l} \tag{A1}$$

where

$$\xi_1 = 1 + \left(1 + nR + \frac{b_a}{b_w}\right) r_b r_t \tag{A2}$$

with

$$r_b = \frac{b_w}{b_s}, \quad r_t = \frac{t_w}{t_s}, \quad R = \frac{b_f}{b_w}\frac{t_f}{t_w}$$

and

n = 0 for integral-stiffened panels
n = 1 for zee- and integral-zee-stiffened panels
n = 2 for integral-tee-stiffened panels

The distance from the neutral surface of the plate-stiffener combination to the middle surface of the skin is

$$y_o = b_w \xi_2 \tag{A3}$$

where

$$\xi_2 = \frac{(1 + 2nR)r_b r_t}{2\xi_1} \tag{A4}$$

The radius of gyration of the panel cross section is

$$\rho = b_w \xi_3 \tag{A5}$$

where

$$\xi_3 = \left\{ \frac{r_b r_t \left[ (4 + 12nR)\left(1 + r_b r_t \frac{b_a}{b_w}\right) + (1 + 4nR) r_b r_t \right]}{12\xi_1^2} \right\}^{1/2} \tag{A6}$$

## Design Stresses

It is assumed in this analysis that the moment resulting from the eccentricities and lateral pressure produces compression in the skin of the panel. To calculate the maximum compressive stress which occurs in the skin, the secant formula (eq. (8)) for columns with an eccentric end load can be expressed in nondimensional form by using the previously defined geometric properties, as

$$\frac{\sigma}{E} = \frac{N_x/E\ell}{\bar{t}/\ell}\left[1 + \frac{e}{\ell}\frac{\ell}{b_w}\frac{\xi_2}{\xi_3^2}\sec\left(\frac{\ell}{b_w}\frac{1}{2\xi_3}\sqrt{\frac{N_x/E\ell}{\bar{t}/\ell}}\sqrt{\frac{1}{\eta_g}}\right)\right] \tag{A7}$$

The plasticity reduction factor $\eta_g$ would be difficult to determine for eccentrically loaded columns. Herein, the plasticity reduction factor for columns with no eccentricity of loading is used. This reduction is given by the ratio of the tangent modulus to Young's modulus of the material

$$\eta_g = \frac{E_T}{E} \tag{A8}$$

The value for the tangent modulus is taken at the maximum stress in the eccentrically loaded column; hence, by using equation (A8) conservative results can be obtained.

The local buckling stress of the skin between stiffeners, including the restraint of the stiffeners, is expressed as

$$\frac{\sigma}{E} = \frac{\eta_l k\pi^2}{12(1 - \mu^2)}\left(\frac{t_s}{b_s}\right)^2 \tag{A9}$$

The plasticity reduction factor for local buckling $\eta_l$ is taken to be

$$\eta_l = \frac{E_S}{E}\left(\frac{1}{2} + \frac{1}{2}\sqrt{\frac{1}{4} + \frac{3}{4}\frac{E_T}{E_S}}\right) \tag{A10}$$

which is derived in reference 7 for plates that are simply supported along their unloaded edges.

## Designs for Stress Below Proportional Limit of Material

Parameter optimization.- For designs with stresses below the proportional limit of the material, $\eta_g = \eta_l = 1$. The maximum stress which occurs in the skin, given by the secant formula (eq. (A7)), is equated to the local-buckling stress of the skin (eq. (A9)). By solving for $t_s$ from the resulting equation and substituting this variable into equation (A1), the following equation is obtained:

$$\frac{\bar{t}}{l} = \frac{1}{r_b}\frac{b_w}{l}\xi_1\left\{\frac{12(1 - \mu^2)}{k\pi^2}\frac{N_x/El}{\bar{t}/l}\left[1 + \alpha\frac{l}{b_w}\sec\left(\beta\frac{l}{b_w}\right)\right]\right\}^{1/2} \tag{A11}$$

where

$$\alpha = \frac{e}{l}\frac{\xi_2}{\xi_3^2} \tag{A12}$$

and

$$\beta = \frac{1}{2\xi_3}\sqrt{\frac{N_x/El}{\bar{t}/l}} \tag{A13}$$

Equation (A11) is given in terms of the loading parameter $N_x/El$, equivalent-thickness parameter $\bar{t}/l$, eccentricity parameter $e/l$, and geometric proportions of the panel. The usual practice in mass-strength analyses is to determine the geometric proportions that minimize $\bar{t}/l$ while $N_x/El$ is held constant or that maximize $N_x/El$ while $\bar{t}/l$ is held constant. The form of equation (A11) does not lend itself to this approach, but the desired geometric proportions can be obtained by minimizing $\bar{t}/l$ while the ratio

$\frac{N_x}{E\ell}\Big/\frac{\bar{t}}{\ell}$ is held constant. The values of $\mu$, n, R, $b_a/b_w$, and $e/\ell$ are fixed for a given case, and the ratios $\ell/b_w$, $r_b$, and $r_t$ are varied to determine the minimum-mass panel proportions.

The first ratio considered is $\ell/b_w$. Equation (A11) can be written as

$$\frac{\bar{t}}{\ell} = H\left(\frac{\ell}{b_w}\right)^{-1}\left[1 + \alpha\,\frac{\ell}{b_w}\sec\left(\beta\,\frac{\ell}{b_w}\right)\right]^{1/2} \tag{A14}$$

where $H = \frac{\xi_1}{r_b}\left[\frac{12(1-\mu^2)}{k\pi^2}\,\frac{N_x/E}{\bar{t}/\ell}\right]^{1/2}$ and H, $\alpha$, and $\beta$ are not functions of $\ell/b_w$. To obtain the ratio $\ell/b_w$ which gives minimum $\bar{t}/\ell$, the derivative $\frac{\partial(\bar{t}/\ell)}{\partial(\ell/b_w)}$ is equated to zero yielding

$$-2\cos^2\theta + \frac{\alpha}{\beta}\left(-\theta\cos\theta + \theta^2\sin\theta\right) = 0 \tag{A15}$$

where

$$\theta = \beta\,\frac{\ell}{b_w} \tag{A16}$$

The solution of the transcendental equation (A15) is shown graphically in figure 12. It is convenient now to consider equation (A11) as a function of the two variables $r_b\sqrt{k}$ and $r_b r_t$ ($\alpha$, $\beta$, and hence $\theta$ are only functions of $r_b r_t$). Maximum efficiency is then obtained when $r_b\sqrt{k}$ is a maximum for a given value of $r_b r_t$. The maximum value of $r_b\sqrt{k}$ can be obtained from the local-buckling-coefficient data of reference 5. As an example, the plot necessary to provide this information for the integral-tee-stiffened panel under uniform compression is shown in figure 13. This plot was prepared by selecting a value of $r_b r_t$ and trying a range of $r_t$ until the maximum $r_b\sqrt{k}$ was found. The dashed line separates the region of the graph where skin buckling is restrained by the stiffeners from the region where stiffener buckling is restrained by the skin. Maximum values of $r_b\sqrt{k}$ occur in the region of panel proportions where stiffener buckling is restrained by the skin for a uniformly stressed cross section.

In this analysis the stress is not uniform but is a sum of the uniform direct stress and the stress resulting from the moment produced by the eccentricities or lateral pressure. Since local-buckling equations which account for the effects of an applied moment are not available, the local-buckling behavior is based on the assumption that the maxi-

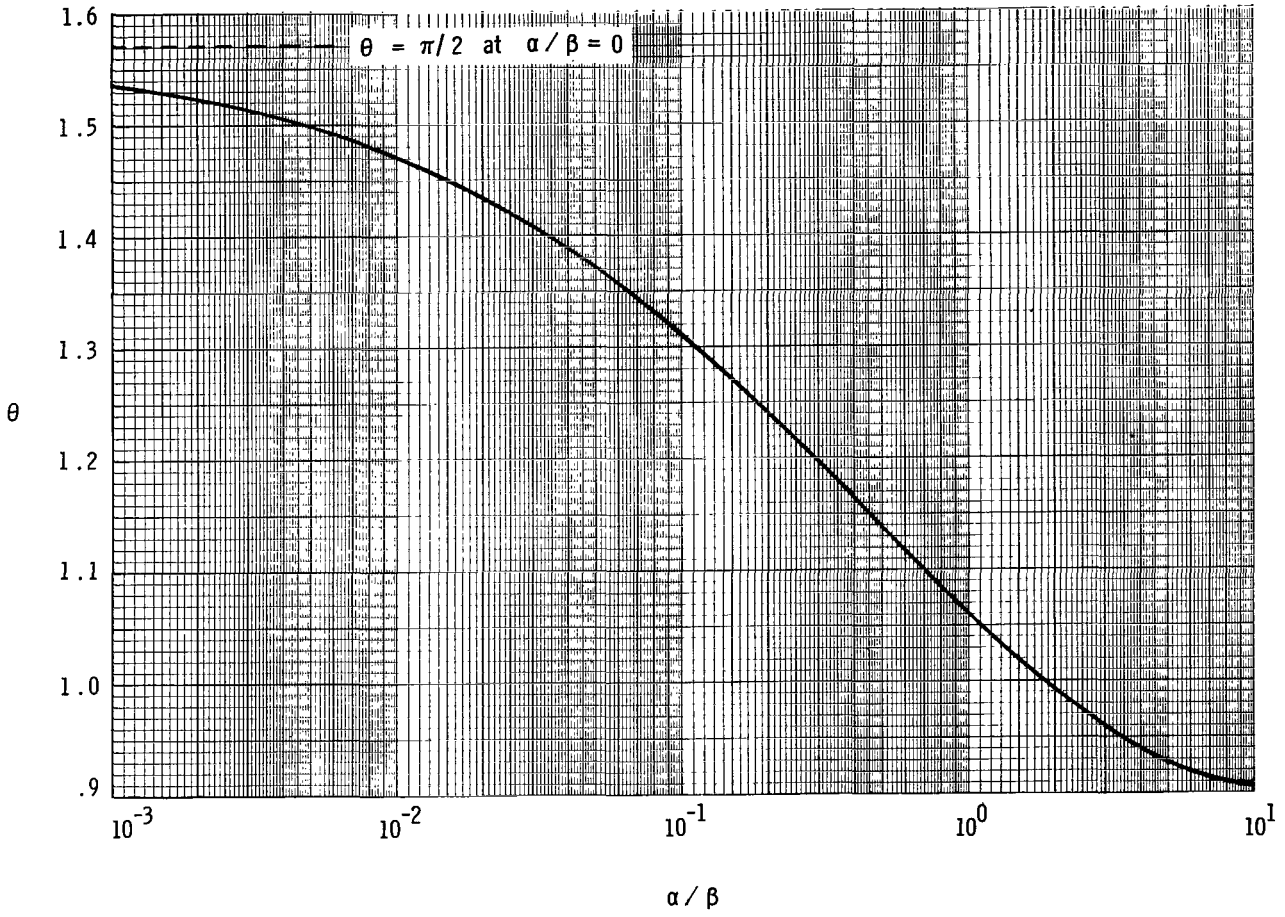


Figure 12.- Solution of transcendental equation (A15) used for determining optimum ratio of stiffener depth to panel length $b_w/l$ for eccentrically loaded panels.

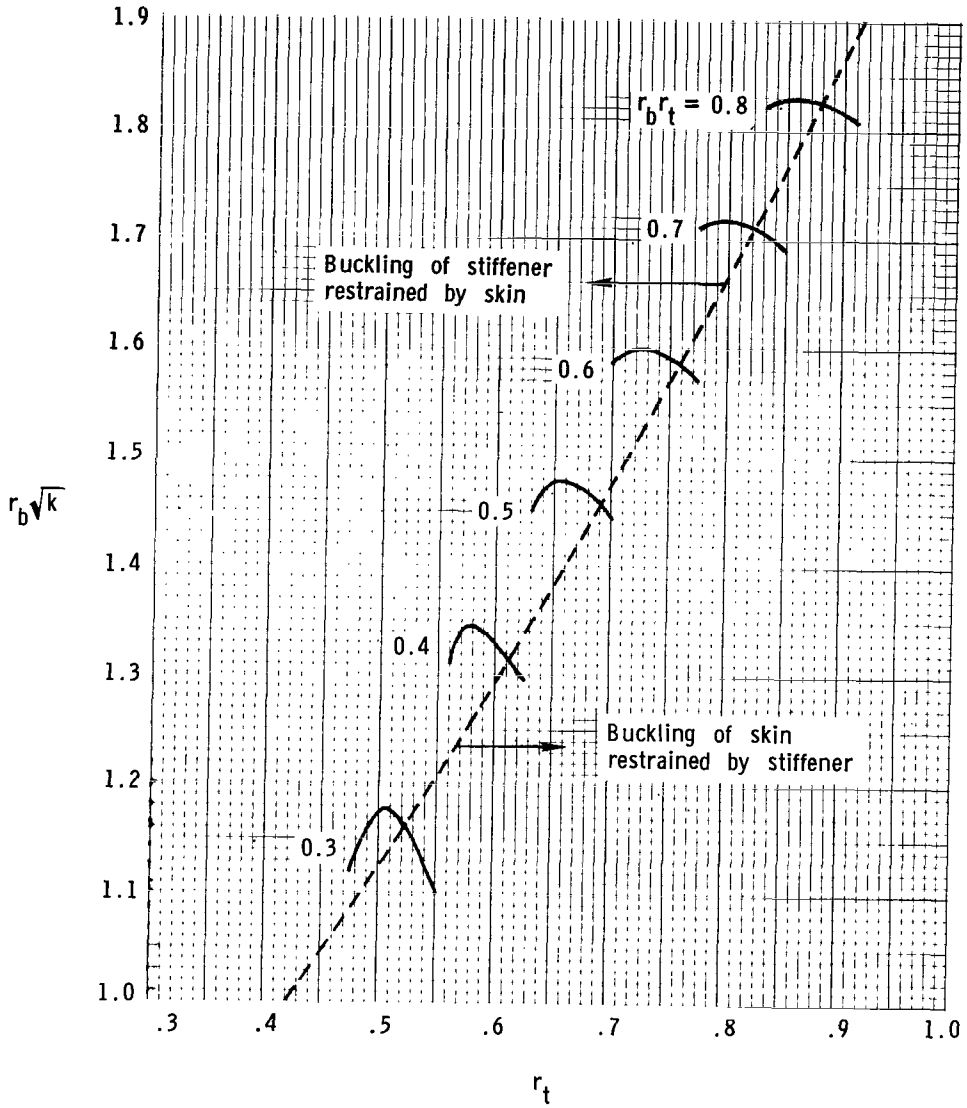


Figure 13.- Local-buckling relationships for integral-tee-stiffened panels. $\frac{b_f}{b_w} = 0.3$; $\frac{t_f}{t_w} = 1.0$.

mum stress which occurs in the skin is applied uniformly to the cross section. This assumption is conservative since the stiffeners would actually be at a stress below the maximum; and hence, the panel would have a higher local-buckling strength than assumed. In view of this conservative assumption, the panel proportions corresponding to the maximum value of $r_b\sqrt{k}$ on the constant $r_b r_t$ curves are used for design in this investigation. Resulting curves of $r_b\sqrt{k}$ versus $r_b r_t$ are shown in figure 14.

Procedure for generating mass-strength curves.- The procedure used to generate the parts of the mass-strength curves, shown in figures 5 to 7, that are for panel designs with stresses below the material proportional limit is as follows:

(1) Select $e/l$, $\frac{N_x}{El}\Big/\frac{\bar{t}}{l}$, $b_f/b_w$, and $t_f/t_w$.

(2) Try a range of values of $r_b r_t$ and corresponding maximum values of $r_b\sqrt{k}$ from figure 14. Calculate $\alpha$ and $\beta$ from equations (A12) and (A13), respectively.

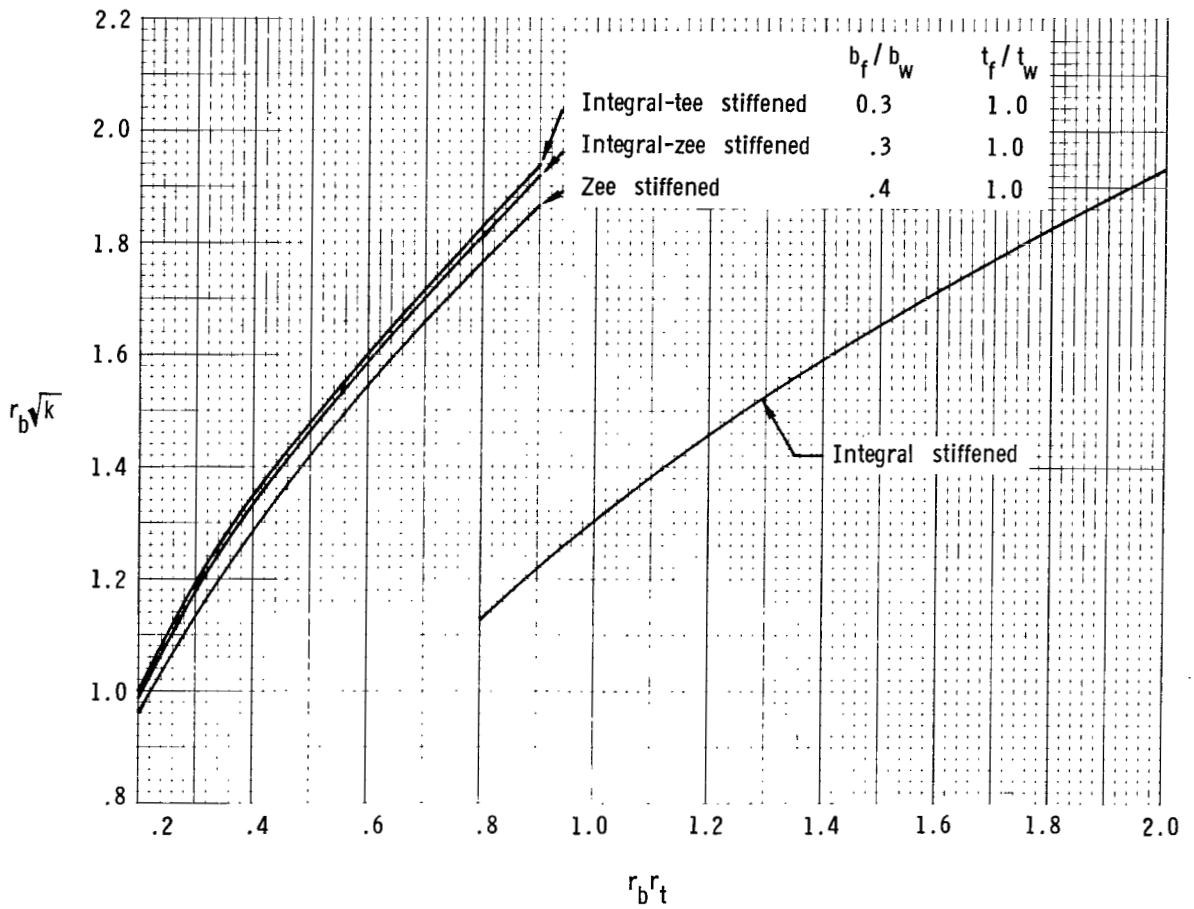


Figure 14.- Maximum $r_b\sqrt{k}$ for stiffened panels obtained from local buckling relationships as shown in figure 13.

(3) Solve for $\theta$ from the transcendental equation (A15) or figure 12, and then determine $l/b_w$ from equation (A16).

(4) Calculate $\bar{t}/l$ from equation (A11) and select the minimum $\bar{t}/l$ for the range of $r_b r_t$.

(5) By using $\frac{N_x}{El} = \frac{N_x/El}{\bar{t}/l}\frac{\bar{t}}{l}$, a point $\left(\frac{N_x}{El}, \frac{\bar{t}}{l}\right)$ can be obtained.

(6) Repeat this entire procedure for different values of $e/l$ and $\frac{N_x}{El}\Big/\frac{\bar{t}}{l}$ until the desired curve is generated.

The related curves giving the geometric proportions $r_b$ and $r_t$ versus the eccentricity parameter $e/l$ are given in figures 9 and 10. The changes in these geometric proportions that occurred as $N_x/El$ was varied throughout the design range were found to be insignificant.

Procedure for determining panel dimensions.- To determine the cross-sectional dimensions of a given panel, the following procedure is used:

(1) Specify the load $N_x$, Young's modulus $E$, panel length $l$, equivalent-eccentricity parameter $\phi$, and geometric ratios $b_a/b_w$, $b_f/b_w$, and $t_f/t_w$. $\left(\text{Values of } \frac{b_f}{b_w} = 0.3 \text{ and } \frac{t_f}{t_w} = 1.0 \text{ were used for the curves shown in figures 5 to 7.}\right)$

(2) Determine $\bar{t}/l$ from figure 5, 6, or 7; $r_b$ from figure 9; $r_t$ from figure 10; $\xi_1, \xi_2, \xi_3$ from equations (A2), (A4), (A6), respectively; $\alpha$ and $\beta$ from equations (A12) and (A13), respectively; and $\theta$ from figure 12.

Then $t_s$, $t_w$, $b_w$, and $b_s$ are obtained from the following design equations:

$$t_s = \frac{\bar{t}}{l}\frac{l}{\xi_1} \tag{A17}$$

$$t_w = r_t t_s \tag{A18}$$

$$b_w = \frac{l\beta}{\theta} \tag{A19}$$

$$b_s = \frac{b_w}{r_b} \tag{A20}$$

## Designs for Stress Above Proportional Limit of Material

Procedure for generating mass-strength curves.- The analysis in this section is used for designs when the maximum stress is above the proportional limit of the material. In this analysis the design stresses are combined in a different manner from the condition

of stresses below the proportional limit. The local-buckling stress given by equation (A9) can be combined with equation (A1) to give $l/b_w$ as

$$\frac{l}{b_w} = \sqrt{\frac{\sigma}{\eta_l E}} \frac{\sqrt{12(1 - \mu^2)}}{\pi} \frac{1}{r_b\sqrt{k}} \frac{\xi_1}{\bar{t}/l} \tag{A21}$$

By substituting $l/b_w$ from equation (A21) into equation (A7) and rearranging, the following equation is obtained:

$$\left(\frac{\bar{t}}{l}\right)^2 + B\frac{\bar{t}}{l} - \frac{\sigma/E}{\frac{N_x/El}{(\bar{t}/l)^3}} = 0 \tag{A22}$$

where

$$B = B_1 \frac{e}{l} \frac{\xi_2}{\xi_3} \sec\left(\frac{B_1}{2}\sqrt{\frac{N_x/El}{(\bar{t}/l)^3}}\sqrt{\frac{1}{\eta_g}}\right) \tag{A23}$$

and

$$B_1 = \sqrt{\frac{\sigma}{\eta_l E}} \frac{\sqrt{12(1 - \mu^2)}}{\pi} \frac{1}{r_b\sqrt{k}} \frac{\xi_1}{\xi_3} \tag{A24}$$

The parameter $\bar{t}/l$ can be determined from equation (A22) for a given stress $\sigma$ and corresponding material properties $E$, $E_T$, and $E_S$, eccentricity parameter $e/l$, the ratio $\frac{N_x}{El}\Big/\left(\frac{\bar{t}}{l}\right)^3$, and the geometric proportions of the cross section. Various combinations of these parameters must be examined to determine points on a mass-strength curve. The following procedure is used to examine these parameters in a systematic manner (see fig. 15):

(1) Select $e/l$, $b_f/b_w$, and $t_f/t_w$.

(2) Select a value of stress $\sigma$

(a) To include plasticity reduction, obtain $E$, $E_T$, and $E_S$ from material stress-strain diagram; then calculate $\eta_g$ and $\eta_l$ from equations (A8) and (A10), respectively.

(b) To neglect plasticity reduction and assume a bilinear stress-strain curve that is perfectly elastic up to the yield point and perfectly plastic thereafter, use $\sigma = \sigma_{cy}$ and $\eta_g = \eta_l = 1$.

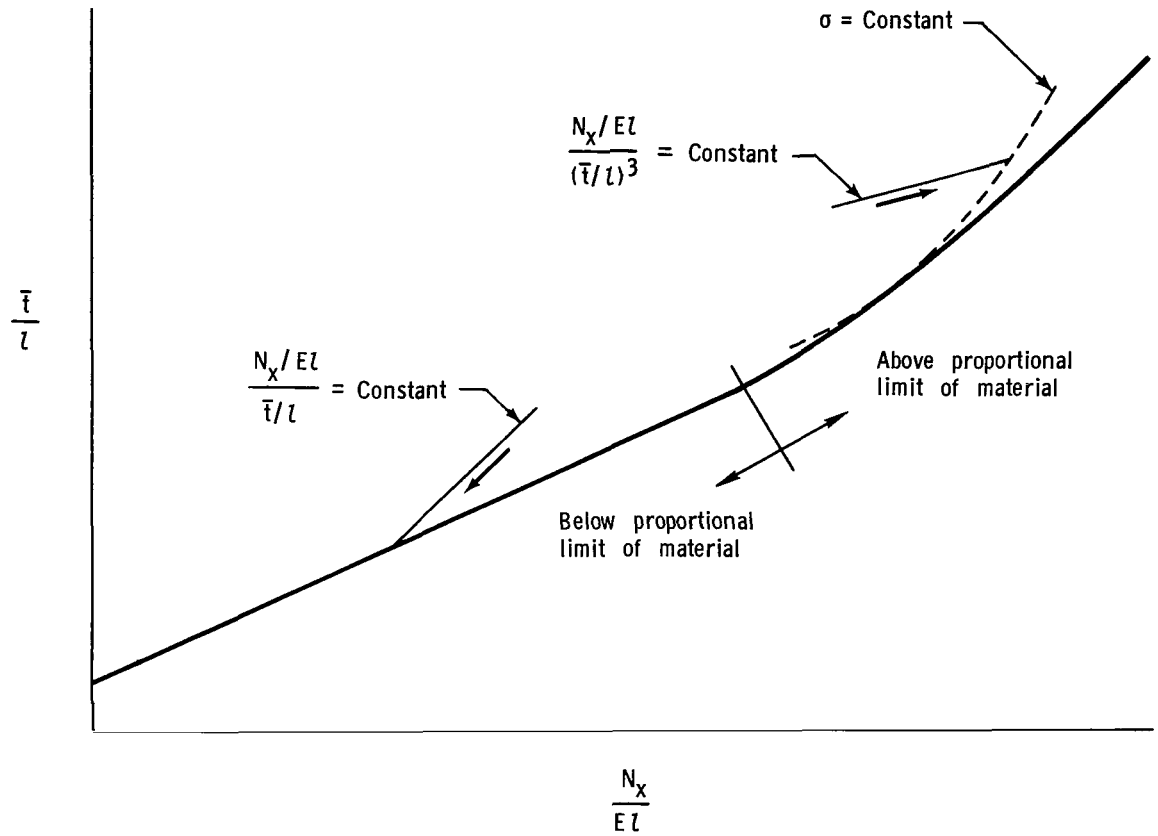


Figure 15.- Typical solution paths for generating mass-strength curves on log-log plots.

(3) Select a constant $\frac{N_x}{El}\Big/\left(\frac{\bar{t}}{l}\right)^3$. This constant establishes a straight line with a slope of 1/3 on the log-log plot in figure 15. The desired design is obtained by determining the geometric proportions of the cross section which give an extremum along this $\frac{N_x}{El}\Big/\left(\frac{\bar{t}}{l}\right)^3$ = Constant line in the direction indicated. Thus, the desired point is established by maximizing $N_x/El$ and corresponding $\bar{t}/l$ along this line. This maximum is determined by varying the parameter $r_b r_t$. Equation (A22) yields a maximum $\bar{t}/l$ when the parameter B is minimized. The parameter B is minimum for a maximum $r_b\sqrt{k}$ at a given $r_b r_t$.

(4) Try a range of values for $r_b r_t$ and corresponding maximum values of $r_b\sqrt{k}$ from figure 14. Determine B and $B_1$ from equations (A23) and (A24), respectively.

(5) Calculate $\bar{t}/l$ from equation (A22), and select the maximum $\bar{t}/l$ for the range of $r_b r_t$. This point is indicated where the $\frac{N_x}{El}\Big/\left(\frac{\bar{t}}{l}\right)^3$ curve coincides with the $\sigma$ = Constant curve in figure 15.

(6) By using $\frac{N_x}{E\ell} = \frac{N_x/E\ell}{(\bar{t}/\ell)^3}\left(\frac{\bar{t}}{\ell}\right)^3$, a point $\left(\frac{N_x}{E\ell}, \frac{\bar{t}}{\ell}\right)$ can be obtained.

(7) Repeat for different values of $\frac{N_x}{E\ell}\Big/\left(\frac{\bar{t}}{\ell}\right)^3$ (lines which are parallel to the one shown in fig. 15) until a curve is generated for the stress $\sigma$ which was selected in step 2. This curve is shown as a dashed line in figure 15.

(8a) If the plasticity reduction is included, several values of stress must be selected resulting in a family of curves whose envelope will be the desired mass-strength curve.

(8b) If the plasticity reduction is neglected, a single curve will be obtained since only the stress $\sigma_{cy}$ is considered.

(9) Repeat this entire procedure for different values of $e/\ell$ until all desired design curves are generated.

The curves relating the geometric proportions $r_b$ and $r_t$ to the eccentricity parameter (see figs. 9 and 10) are also applicable for designs with stresses above the proportional limit. There were some differences between the proportions which gave the theoretical minimum-mass design and the proportions shown in figures 9 and 10. However, the resulting differences in mass of the designs were negligible.

The above procedure can also be used to generate mass-strength curves in the region where stresses are below the material proportional limit. However, the procedure described in this section requires considerably more calculations than the procedure described in the previous section, which was tailored for use below the proportional limit. The procedure for use below the proportional limit involves solution paths along constant $\frac{N_x}{E\ell}\Big/\frac{\bar{t}}{\ell}$ lines shown in figure 15. The desired design is obtained by determining the geometric proportions of the cross section which give an extremum along this $\frac{N_x}{E\ell}\Big/\frac{\bar{t}}{\ell}$ = Constant line in the direction indicated. Hence, for this region the desired point is established by minimizing $\bar{t}/\ell$ and corresponding $N_x/E\ell$ along this line.

Procedure for determining panel dimensions.- To determine the cross-sectional dimensions of the panels for a given case the following procedure is used:

(1) Specify load $N_x$, Young's modulus $E$, panel length $\ell$, equivalent-eccentricity parameter $\phi$, and geometric ratios $b_a/b_w$, $b_f/b_w$, and $t_f/t_w$. (Values of $\frac{b_f}{b_w} = 0.3$ and $\frac{t_f}{t_w} = 1.0$ were used for the curves shown in figures 5 to 7.)

(2) Determine $t/\ell$ from figure 5, 6, or 7; $r_b$ from figure 9; $r_t$ from figure 10; $\xi_1$ from equation (A2); and $r_b\sqrt{k}$ from figure 14.

Then $t_s$ and $t_w$ are obtained from design equations (A17) and (A18), respectively:

$$t_s = \frac{\bar{t}}{l}\frac{l}{\xi_1}$$

$$t_w = r_t t_s$$

Next, a value of stress $\sigma$ is selected and corresponding values of $E_T$ and $E_S$ are obtained from a stress-strain diagram. The plasticity reduction factors $\eta_g$ and $\eta_l$ are determined from equations (A8) and (A10), respectively. Then $b_w$ can be obtained from the expression

$$b_w = \frac{l\pi\frac{\bar{t}}{l} r_b\sqrt{k}}{\sqrt{\frac{\sigma}{\eta_l E}}\sqrt{12\left(1-\mu^2\right)}\xi_1} \tag{A25}$$

Stress $\sigma$ is calculated by using equation (A7). If the plasticity reduction is included, an iteration will be required to make the calculated stress $\sigma$ agree with the selected value. If the plasticity reduction is neglected, $\sigma = \sigma_{cy}$ is selected with $\eta_g = \eta_l = 1$, and no iteration on the stress is required since only a single value of compressive-yield stress is considered on the mass-strength curve. Finally, $b_s$ is determined from equation (A20):

$$b_s = \frac{b_w}{r_b}$$

Load Applied Through Neutral Surface

For no eccentricity, equation (A12) gives $\alpha = 0$, and the corresponding value of $\theta$ from equation (A15) is $\theta = \frac{\pi}{2}$. Using equations (A13) and (A16), equation (A11) reduces to

$$\frac{\bar{t}}{l} = \frac{\sqrt{12\left(1-\mu^2\right)}\xi_1}{\pi^2 r_b\sqrt{k}\,\xi_3}\frac{N_x/El}{\bar{t}/l} \tag{A26}$$

or

$$\frac{N_x}{El} = \epsilon\left(\frac{\bar{t}}{l}\right)^2 \tag{A27}$$

where

$$\epsilon = \frac{\pi 2 r_b \sqrt{k}\, \xi_3}{\sqrt{12(1 - \mu^2)\xi_1}} \tag{A28}$$

Numerical values for the structural efficiency factor $\epsilon$ obtained using equation (A28) agree closely with the corresponding values given in reference 1.

## REFERENCES


1. Emero, Donald H.; and Spunt, Leonard: Wing Box Optimization Under Combined Shear and Bending. J. Aircraft, vol. 3, no. 2, Mar.-Apr. 1966, pp. 130-141.

2. Shanley, Francis R.: Optimum Design of Eccentrically Loaded Columns. J. Struct. Div., Amer. Soc. Civil Eng., vol. 93, no. ST4, Aug. 1967, pp. 201-226.

3. Timoshenko, Stephen P.; and Gere, James M.: Theory of Elastic Stability. Second ed., McGraw-Hill Book Co., Inc., 1961.

4. Bleich, Friedrich: Buckling Strength of Metal Structures. McGraw-Hill Book Co., Inc., 1952.

5. Becker, Herbert: Handbook of Structural Stability. Part II – Buckling of Composite Elements. NACA TN 3782, 1957.

6. Hickman, William A.; and Dow, Norris F.: Direct-Reading Design Charts for 75S-T6 Aluminum-Alloy Flat Compression Panels Having Longitudinal Extruded Z-Section Stiffeners. NACA TN 2435, 1952.

7. Stowell, Elbridge Z.: A Unified Theory of Plastic Buckling of Columns and Plates. NACA Rep. 898, 1948. (Supersedes NACA TN 1556.)

8. Anderson, Roger A.; and Anderson, Melvin S.: Correlation of Crippling Strength of Plate Structures With Material Properties. NACA TN 3600, 1956.

*"The aeronautical and space activities of the United States shall be conducted so as to contribute . . . to the expansion of human knowledge of phenomena in the atmosphere and space. The Administration shall provide for the widest practicable and appropriate dissemination of information concerning its activities and the results thereof."*

—NATIONAL AERONAUTICS AND SPACE ACT OF 1958

# NASA SCIENTIFIC AND TECHNICAL PUBLICATIONS

TECHNICAL REPORTS: Scientific and technical information considered important, complete, and a lasting contribution to existing knowledge.

TECHNICAL NOTES: Information less broad in scope but nevertheless of importance as a contribution to existing knowledge.

TECHNICAL MEMORANDUMS: Information receiving limited distribution because of preliminary data, security classification, or other reasons.

CONTRACTOR REPORTS: Scientific and technical information generated under a NASA contract or grant and considered an important contribution to existing knowledge.

TECHNICAL TRANSLATIONS: Information published in a foreign language considered to merit NASA distribution in English.

SPECIAL PUBLICATIONS: Information derived from or of value to NASA activities. Publications include conference proceedings, monographs, data compilations, handbooks, sourcebooks, and special bibliographies.

TECHNOLOGY UTILIZATION PUBLICATIONS: Information on technology used by NASA that may be of particular interest in commercial and other non-aerospace applications. Publications include Tech Briefs, Technology Utilization Reports and Technology Surveys.

***Details on the availability of these publications may be obtained from:***

**SCIENTIFIC AND TECHNICAL INFORMATION OFFICE**

**NATIONAL AERONAUTICS AND SPACE ADMINISTRATION**

**Washington, D.C. 20546**